www.sciencemag.org/cgi/content/full/science.aau7230/DC1

Supplementary Material for

A degenerate Fermi gas of polar molecules

Luigi De Marco, Giacomo Valtolina, Kyle Matsuda, William G. Tobias, Jacob P. Covey, Jun Ye*

*Corresponding author. Email: ye@jila.colorado.edu

Published 17 January 2019 as *Science* First Release
DOI: 10.1126/science.aau7230

This PDF file includes:

Supplementary Materials

Materials and Methods

Preparation of degenerate atomic species. In an atomic vapor cell ($P \sim 10^{-7}$ torr), a dual species magneto-optical trap (MOT) cools and traps Rb and K atoms. Once the MOT is fully loaded, a compressed MOT stage further cools the atoms, which is followed by sub-Doppler cooling. Both bright and Λ–enhanced gray molasses are sequentially performed on the D_2 transition of Rb for 2 and 8 ms, respectively, and the atoms reach a final temperature of 10 μK. Simultaneously, Λ–enhanced gray molasses is performed for 10 ms on the D_1 transition of K, which reaches a final temperature of 20 μK. After reloading the atoms into the quadrupole field, adiabatic compression raises their temperature to 100 μK, and 1×10^9 Rb and 7×10^7 K are captured in the $|F, m_F\rangle = |2, 2\rangle$ and $|9/2, 9/2\rangle$ states, respectively.

Atoms are spatially transported ~1 m to a high-vacuum science cell ($P \sim 10^{-11}$ torr) by physically translating the anti-Helmholtz coils producing the quadrupole field. The quadrupole trap is plugged with a blue-detuned beam (20 μm waist, 760 nm), and magnetic evaporation is performed with a chirped driving of the $|2, 2\rangle \longrightarrow |1, 1\rangle$ transition of Rb using a microwave horn at 6.8 GHz. Potassium is sympathetically cooled, and at the end of magnetic evaporation, 6×10^6 of each species remain at 4 μK.

Once magnetic evaporation is complete, a crossed optical dipole trap (xODT) is turned on to capture the cold atoms, and the quadrupole field and plug beam are ramped off while a bias field of 30 G is turned on. The xODT is formed by two elliptical beams at 1064 nm with waists of 45 × 170 μm crossing at 45°. Optical evaporation is performed by exponentially ramping the beams to variable cuts (~1/10 of their initial value) and then recompressing the trap such that the K trap frequencies are $(\omega_x, \omega_y, \omega_z) = 2\pi \times (45, 250, 80)$ Hz. Depending on the final trap depth, the atom number and temperature can be varied significantly. Typically, 10^6 Rb and 1.4×10^6 K atoms at 300 nK, or 7×10^4 Rb and 5×10^5 K atoms at 50 nK can be produced.

During optical evaporation the atoms are transferred to the Feshbach states using adiabatic rapid passage (ARP). Rubidium is transferred from $|2, 2\rangle \longrightarrow |1, 1\rangle$ and K from $|9/2, 9/2\rangle \longrightarrow |9/2, -9/2\rangle$; each is transferred with about 98% efficiency and untransferred atoms are blasted out of the trap with resonant light. Once optical evaporation and state transfer are complete, the bias field is ramped to 550 G in preparation for molecule production. The progression of atom numbers and temperature throughout the experimental cycle is shown in Fig. S1.

Production and imaging of ground state KRb. In order to prevent gravitational sag from inducing oscillations in the ground-state molecules, a vertical lattice formed by two counter-propagating beams (170 μm waist, 1064 nm) is adiabatically ramped on. It is found that a lattice depth of 30 E_r^{Krb} is sufficient to suppress the effects of gravitational sag. Once molecules are produced, the lattice is ramped off in 5 ms.

In the corrugated trap, weakly bound Feshbach molecules are produced by sweeping the magnetic field through the Fano–Feshbach resonance at 546.6 G. The field is swept from 556 G to 545.6 G in 3 ms. Conversion from unbound atoms to Feshbach molecules varies significantly depending on the initial temperature of the atoms, and it can be as high as 50% at low temperature and as low as 15% at high temperature.

Molecules are transferred to the rovibronic ground state using stimulated Raman adiabatic passage (STIRAP). The two STIRAP lasers, which operate at 968 nm and 689 nm, are each locked to a common high-finesse optical cavity using the Pound–Drever–Hall method. The STIRAP sequence is 4 μs long, and has a transfer efficiency of ~90%; the reported molecule numbers are corrected for this efficiency.

Immediately after molecule production, unpaired atoms are removed from the trap to mitigate molecule loss. To remove K, a 30 μs pulse of resonant light is applied to blast K out of the trap while leaving the molecules unaffected. To remove leftover Rb, which is in the $|1, 1\rangle$ state, four ARP + blast sequences are applied to ensure the total removal of Rb. The molecule number and temperature are found to be unaffected by the atom removal, which corroborates our expectation that KRb + KRb reaction products are ejected from the trap without affecting the remaining molecules.

To image molecules, the xODT is diabatically turned off and the STIRAP sequence is reversed to produced Feshbach molecules once again. The magnetic field is then jumped across the resonance to dissociate the weakly bound molecules into free atoms and the K atoms are imaged on the |9/2, 9/ 2⟩ ⟶ |11/2, -11/2⟩' cycling transition after a variable amount of time of flight. We may also image Feshbach molecules directly without dissociation by using resonant light to separate the molecules into free atoms. In this case, we must account for the reduced absorption cross section compared to free atoms, which we find to be about 0.7 times smaller.

Image Fitting. The molecular cloud is imaged from the side at an angle of θ = 22.5° with respect to the principal axes of the trap. The imaging axes are

$$\hat{x}_1 = \frac{\hat{x}\sin\theta + \hat{z}\cos\theta}{\sqrt{2}} \tag{S1a}$$

$$\hat{x}_2 = \hat{y}. \tag{S1b}$$

The 2D column density distributions are fit to either a Maxwell–Boltzmann distribution for $T/T_F \sim 1$ or a Fermi–Dirac distribution for $T/T_F \ll 1$.

For the Maxwell–Boltzmann distribution, we fit to

$$n_{\mathrm{Cl}} = n_0 e^{-\frac{1}{2}\left(\frac{x_1^2}{\sigma_1^2} + \frac{x_2^2}{\sigma_2^2}\right)} + c, \tag{S2}$$

with n_0, $\{\sigma_i\}$, and c as fitting parameters. Respectively, these are the peak density, the size of the cloud along each imaging axis, and the imaging offset. The cloud sizes are related to the classical temperature of the gas via

$$\sigma_i = \frac{\sqrt{1 + (\omega_i \tau)^2}}{\omega_i} \sqrt{\frac{k_{\mathrm{B}} T}{m}}, \tag{S3}$$

where k_B is Boltzmann's constant, m = 127 amu is the molecular mass, ω_i is the trap frequency along the i^{th} direction, and τ is the time of flight.

For the Fermi–Dirac distribution, we make the Thomas–Fermi approximation and fit to

$$n_{\mathrm{FD}} = -n_0 \mathrm{Li}_2\left(-z e^{-\frac{1}{2}\left(\frac{x_1^2}{\sigma_1^2} + \frac{x_2^2}{\sigma_2^2}\right)}\right) + c. \tag{S4}$$

Here, z is the fugacity, which is a fitting parameter in addition to those described above, and $\mathrm{Li}_s(z)$ is the polylogarithm function. The quantity T/T_F is determined solely by the fugacity according to

$$\left(\frac{T}{T_F}\right)^3 = -\frac{1}{6\mathrm{Li}_3(-z)} \tag{S5}$$

Azimuthal averaging for Fig. 2 is carried out by converting the image from Cartesian coordinates ($\hat{x}_1$and $\hat{x}_2$) to polar coordinates (r and ϕ) and averaging over the ϕ variable. Fitting of the momentum distributions is done before azimuthal averaging, and the data and fits are averaged separately.

Density loss fitting. In a classical, harmonically trapped gas, the *in situ* average density is given by

$$n(T) = \frac{N}{V} = \frac{N}{8\pi^{3/2}} \bar{\omega}^3 \left(\frac{k_B T}{m}\right)^{-3/2}, \tag{S6}$$

where $\bar{\omega} = (\omega_1\omega_2\omega_3)^{1/3}$ is the geometric mean trap frequency. Differentiation of the above equation with respect to time yields Eq. 1, with $\dot{N} = -\beta n^2 V$ being the rate at which particles are lost.

Since, according to the Bethe–Wigner threshold law, the two-body rate constant is proportional to temperature, it is convenient to write $\beta = bT$, with b independent of temperature. Then, the rate equation reads

$$\frac{\mathrm{d}n}{\mathrm{d}t} = -bTn^2 - \frac{3}{2}\frac{n}{T}\frac{\mathrm{d}T}{\mathrm{d}t}. \tag{S7}$$

While, in principle, anti-evaporation is the main source of heating, we observe a linear increase in temperature over the course of the hold time of the molecules; an example of which is shown in Fig. S2a. We therefore do not fit T, but measure it to be $T = T_0 + ht$, where h is the heating rate and t is the hold time. With this, Eq. S7 becomes

$$\frac{\mathrm{d}n}{\mathrm{d}t} = -b(T_0 + ht)n^2 - \frac{3}{2}n\frac{h}{T_0 + ht}. \tag{S8}$$

The closed form solution for Eq. S8 is

$$n(t) = \frac{n_0 h T_0^{3/2}}{(ht + T_0)\left(2n_0 T_0^2\left(\sqrt{T_0} - \sqrt{ht + T_0}\right)b + h\left(\sqrt{ht + T_0} + 2n_0 T_0^{3/2} b\right)\right)}, \tag{S9}$$

and density loss curves are fit to this equation. Example density loss curves and their corresponding fits are shown in Fig. 3b.

In our analysis, b and n_0 are fitting parameters, while T_0 and h are measured. T_0 is measured at time $t = 0$ by averaging 3–5 images and fitting to the Fermi–Dirac distribution, while h is measured by considering the increase in $\sigma_i^2 \propto T$ as a function of time. Despite the heating, molecular degeneracy is preserved over the course of the molecules' lifetime, as shown in Fig. S2b.

In Figs. 4a and 4b, the quantities plotted are $\beta = bT_0$ and $b = \beta/T$, respectively.

Density Fluctuations in an Ideal Fermi Gas

Within the Thomas–Fermi approximation, the density distribution of the ideal Fermi gas is given by

$$n(\boldsymbol{r}) = -\frac{1}{\Lambda^3}\mathrm{Li}_{3/2}\left(-ze^{-\beta V(\boldsymbol{r})}\right). \tag{S10}$$

In the grand canonical ensemble, fluctuations in density are described in the thermodynamic limit by

$$\delta n(\boldsymbol{r})^2 = \langle n^2(\boldsymbol{r})\rangle - \langle n(\boldsymbol{r})\rangle^2 = \frac{1}{\beta}\frac{\partial n(\boldsymbol{r})}{\partial \mu} = -\frac{1}{\Lambda^3}\mathrm{Li}_{1/2}\left(-ze^{-\beta V(\boldsymbol{r})}\right). \tag{S11}$$

Local relative number fluctuations are therefore described by

$$\frac{\delta n(\boldsymbol{r})^2}{n(\boldsymbol{r})} = \frac{\mathrm{Li}_{1/2}\left(-ze^{-\beta V(\boldsymbol{r})}\right)}{\mathrm{Li}_{3/2}\left(-ze^{-\beta V(\boldsymbol{r})}\right)}. \tag{S12}$$

However, in our experiment, we do not consider reactions locally, but rather globally. Therefore, it is necessary to average over all fluctuations in the trap. The normalized spatial probability distribution is given by

$$f(\boldsymbol{r}) = \frac{n(\boldsymbol{r})}{N} = \Lambda^3 \left(\frac{m\bar{\omega}}{h}\right)^3 \frac{1}{\mathrm{Li}_3(-z)} \mathrm{Li}_{3/2}\left(-ze^{-\beta V(\boldsymbol{r})}\right), \tag{S13}$$

so that the size of fluctuations averaged over the trap is

$$\frac{\langle \delta n(\boldsymbol{r})^2 \rangle}{\langle n(\boldsymbol{r}) \rangle} = \frac{\int d\boldsymbol{r} f(r) \delta n(\boldsymbol{r})^2}{\int d\boldsymbol{r} f(r) n(\boldsymbol{r})} \,. \tag{S14}$$

The average suppression of fluctuations is compared to the suppression of fluctuations in the center of the trap in Fig. S3. It is also clear from Fig. S3 that fluctuations are only suppressed at the edge of the trap (3σ) for $T/T_F < 0.2$, which is consistent with our expectation that chemical reactions are only strongly suppressed at the center.

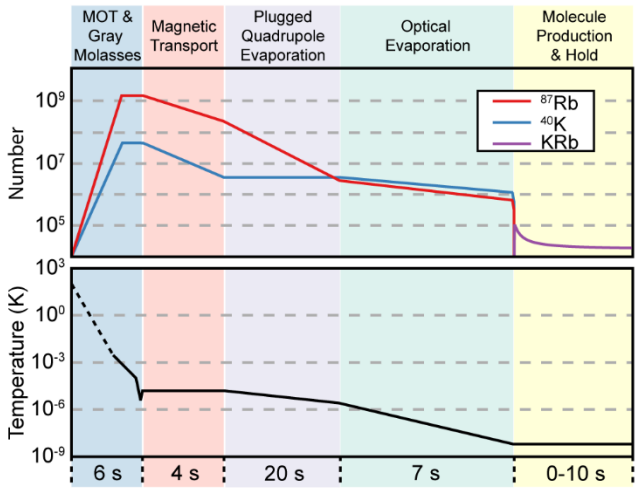

Figure S1: Experimental sequence. The upper panel shows the number of Rb, K, and KRb, while the lower panel shows the temperature of the mixture over the course of the experimental cycle. A single curve is shown for temperature since the atomic species remain thermalized. The time axis is not to scale.

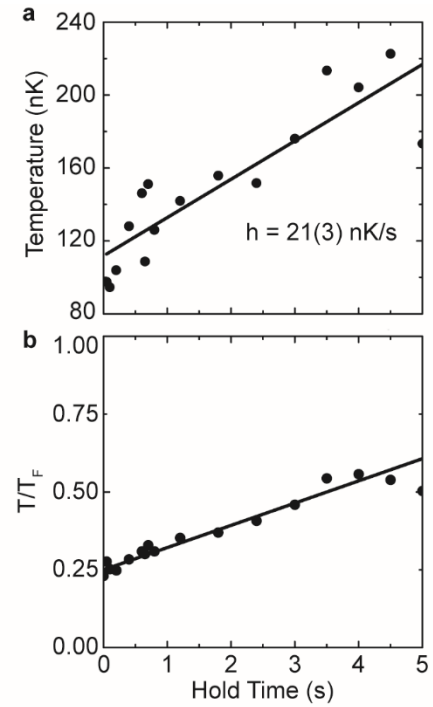

Figure S2: a. Heating Rate. The typical temperature of a molecular gas as a function of time. **b. Degeneracy Loss.** Despite the heating, T/T_F remains small so long as $ht \ll T_0$.

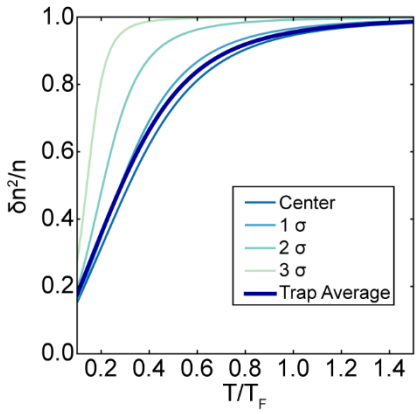

Figure S3: Density Fluctuations in an ideal Fermi gas. Relative density fluctuations in a harmonically trapped Fermi gas at various positions. The bold line corresponds to the average over the trap.